AD_____

GRANT NUMBER DAMD17-98-1-8080

TITLE: Analysis of HRAD1, a Human G2 Checkpoint Control Gene

PRINCIPAL INVESTIGATOR: Blair Besly, Ph.D.
Dr. Scott Davey

CONTRACTING ORGANIZATION: Queen's University
Kingston, Ontario K7L 3N6 Canada

REPORT DATE: July 1999

TYPE OF REPORT: Annual Summary

PREPARED FOR: Commanding General
U.S. Army Medical Research and Materiel Command
Fort Detrick, Maryland 21702-5012

REPORT DOCUMENTATION PAGE

Form Approved
OMB No. 0704-0188

1. AGENCY USE ONLY *(Leave blank)*	2. REPORT DATE	3. REPORT TYPE AND DATES COVERED
	July 1999	Annual Summary (1 Jun 98 – 1 Jul 99)

4. TITLE AND SUBTITLE
Analysis of HRAD1, a Human G2 Checkpoint Control Gene

5. FUNDING NUMBERS
DAMD17-98-1-8080

6. AUTHOR(S)
Blair Besley, Ph.D.
Dr. Scott Davey

7. PERFORMING ORGANIZATION NAME(S) AND ADDRESS(ES)
Queen's University
Kingston, Ontario K7L 3N6 Canada

8. PERFORMING ORGANIZATION REPORT NUMBER

9. SPONSORING / MONITORING AGENCY NAME(S) AND ADDRESS(ES)
U.S. Army Medical Research and Materiel Command
Fort Detrick, Maryland 21702-5012

10. SPONSORING / MONITORING AGENCY REPORT NUMBER

11. SUPPLEMENTARY NOTES

12a. DISTRIBUTION / AVAILABILITY STATEMENT
Approved for Public Release; Distribution Unlimited

12b. DISTRIBUTION CODE

13. ABSTRACT *(Maximum 200 words)*

The purpose of this research is to determine the role of the hRAD1 gene in breast cancer. The reseaqrch includes the generation and analysis of cell lines lacking hRAD1. The analysis includes an assessment of checkpoint proficiency and genomic instability in these cells. The research also includes a biochemical characterization of the hRAD1 protein, including its subcellular localization and protein-protein interactions with other checkpoint proteins. These other checkpoint proteins include BRCA1, hHUS1, and hRAD9. hRAD1 does not interact with BRCA1 but does form a complex with hHUS1 and hRAD9.

14. SUBJECT TERMS				15. NUMBER OF PAGES
Breast Cancer genomic instability, checkpoint, cell cycle, BRCA1				44
				16. PRICE CODE
17. SECURITY CLASSIFICATION OF REPORT	18. SECURITY CLASSIFICATION OF THIS PAGE	19. SECURITY CLASSIFICATION OF ABSTRACT		20. LIMITATION OF ABSTRACT
Unclassified	Unclassified	Unclassified		Unlimited

FOREWORD

Opinions, interpretations, conclusions and recommendations are those of the author and are not necessarily endorsed by the U.S. Army.

____ Where copyrighted material is quoted, permission has been obtained to use such material.

____ Where material from documents designated for limited distribution is quoted, permission has been obtained to use the material.

____ Citations of commercial organizations and trade names in this report do not constitute an official Department of Army endorsement or approval of the products or services of these organizations.

__✓__ In conducting research using animals, the investigator(s) adhered to the "Guide for the Care and Use of Laboratory Animals," prepared by the Committee on Care and use of Laboratory Animals of the Institute of Laboratory Resources, national Research Council (NIH Publication No. 86-23, Revised 1985).

__✓__ For the protection of human subjects, the investigator(s) adhered to policies of applicable Federal Law 45 CFR 46.

__✓__ In conducting research utilizing recombinant DNA technology, the investigator(s) adhered to current guidelines promulgated by the National Institutes of Health.

__✓__ In the conduct of research utilizing recombinant DNA, the investigator(s) adhered to the NIH Guidelines for Research Involving Recombinant DNA Molecules.

____ In the conduct of research involving hazardous organisms, the investigator(s) adhered to the CDC-NIH Guide for Biosafety in Microbiological and Biomedical Laboratories.

Chris Mdell May 31/99

PI - Signature Date

Table of Contents

Introduction

The subject of this research is an analysis of *hRAD1*, a human gene that is homologous to the fission yeast checkpoint control gene *rad1*$^{+}$. This analysis includes the generation of cells lines deficient in *hRAD1* and assessing checkpoint proficiency and genomic instability in these cell lines. The analysis also involves a biochemical characterization of the hRAD1 protein. This characterization consists of the generation of antibodies against hRAD1, determining the subcellular localization of hRAD1, and studying the protein-protein interactions of hRAD1 with other proteins including the BRCA1 protein. The ultimate goal of the research is to determine if *hRAD1* is a tumor suppressor and if *hRAD1* mutations have a role in the pathogenesis of breast cancer.

Progress Report Body

My original grant proposal had five specific aims outlining the objectives of the research. I will addresss each specific aim in turn in the following paragraphs.

Specific Aim 1 is to generate cell lines deficient in *hRAD1*. The first method was to generate mice lacking expression of the mouse gene *mRAD1*. A screen was carried out to obtain genomic clones of the *mRAD1* locus. Five clones were obtained from this screen. However, to date I have not been able to confirm by sequencing that they are from the *mRAD1* locus. The second method was to generate human cell lines deficient in *hRAD1* expression using antisense constructs. I have used both antisense oligonucleotides and stable cell lines expressing antisense *hRAD1* cDNA. In neither case was I able to demonstrate loss of checkpoint control or lack of *hRAD1* expression.

Specific Aim 2 is the analysis of *hRAD1*-deficient cell lines. As reliable cell lines have not been generated this analysis has not been performed in detail. Stable cell lines expressing antisense *hRAD1* cDNA were assessed for their sensitivity to hydroxyurea (HU) and ultraviolet (UV) light. None appeared to be more sensitive than controls. I could not confirm by either Northern or Western blot that the cell lines lacked hRAD1 expression. Therefore, the analysis was not continued. Cell lines transfected with antisense oligonucleotides were analysed for their sensitivity to HU, UV light, and gamma rays. Again, none appeared more sensitive than controls. However, I cannot confirm that these cells lacked hRAD1 expression.

Specific Aim 3 is the generation of antibodies against the hRAD1 protein. The hRAD1 protein was fused to GST and expressed in *E. coli*. The GST-hRAD1 fusion was affinity-purified from *E. coli* extracts using Glutathione-Sepharose beads. The fusion

protein was then injected into two rabbits. Each rabbit was boosted with antigen three times. Blood was collected after each boost for analysis of the serum. The housing, injections, and bleeds of the rabbits were contracted to Cocalico Biologicals Inc. as agreed upon in the grant contract. Polyclonal anti-hRAD1 antibodies were affinity-purified from the rabbit serum. These antibodies reacted specifically with hRAD1 expressed in *E. coli*. However, I am not able to detect endogenous hRAD1 or overexpressed hRAD1 in human cells with these antibodies.

Secific Aim 4 is to determine if hRAD1 interacts with BRCA1, ATR, or ATM. Using neither pull-down experiments with GST-hRAD1, nor co-immunoprecipitation have I been able to detect an interaction between hRAD1 and BRCA1. Possible interactions with ATR and ATM have not been addressed because antibodies against these proteins have not yet been made available to us by our collaborators. I have shown that hRAD1 interacts with hHUS1, which is the human homologue of the fission yeast Hus1 checkpoint control protein. In conjunction with another student in the lab, Bob St. Onge, we have shown that hRAD1 forms a complex with hHUS1 and hRAD9. This work is described in the accompanying manuscript (Appendix 3).

Specific Aim 5 is to determine the subcellular localization of hRAD1 and if it co-localizes with ATR or ATM. This work has been performed by another group.[1] hRAD1 does not co-localize with either ATR or ATM.

[1] Freire, R., Murguia, J.R., Tarsounas, M., Lowndes, N.F., Moens, P.B. and Jackson, S.P. (1998). Human and mouse homologs of *Schizosaccharomyces pombe rad1*$^+$ and *Saccharomyces cerevisiae RAD17*: linkage to checkpoint control and mammalian meiosis. *Genes Dev.* 12: 2560-2573.

Appendix 1 – Key Research Accomplishments

1. The hRAD1 protein interacts with hHUS1.
2. The hRAD1 protein is part of a complex including hHUS1 and hRAD9.

Appendix 2 – Reportable Outcomes

1. We have had a manuscript accepted for publication by Molecular Biology of the Cell. It is currently in press, and a copy of the manuscript is attached as appendix 3.
2. I will receive my Masters of Science degree in July of 1999.

Appendix 3 – Manuscript

St. Onge, R.P., Udell, C.M., Casselman, R. and Davey, S. (1999). The human G2 checkpoint control protein hRAD9 is a nuclear phosphoprotein that forms complexes with hRAD1 and hHUS1. *Mol. Biol. Cell.* In press.

The human G2 checkpoint control protein hRAD9 is a nuclear phosphoprotein that forms complexes with hRAD1 and hHUS1.

Robert P. St. Onge[§], Christian M. Udell[§], Richard Casselman, and Scott Davey[†§‡*]

Cancer Research Laboratories, and Departments of Pathology[§], Oncology[†], and Biochemistry[‡], Queen's University, Kingston, K7L 3N6, Canada.

Running title: The human G2 checkpoint complex.

*Corresponding Author. Botterell Hall, Room A309, Queen's University, Kingston, K7L 3N6, Canada. Telephone (613) 533-6923. FAX (613) 533-6830. Email sd13@post.queensu.ca

Submitted to MBC
5 Jan 99.

Abstract

Eukaryotic cells actively block entry into mitosis in the presence of DNA damage or incompletely replicated DNA. This response in mediated by signal transduction cascades called cell cycle checkpoints. We show here that the human checkpoint control protein hRAD9 physically associates with two other checkpoint control proteins, hRAD1 and hHUS1. Further, hRAD1 and hHUS1 themselves interact, analogously to their fission yeast homologs Rad1 and Hus1. We also show that hRAD9 is present in multiple phosphorylation forms *in vivo*. These phosphorylated forms are present in tissue culture cells that have not been exposed to exogenous sources of DNA damage, but it remains possible that endogenous damage or naturally occurring replication intermediates cause the observed phosphorylation. Finally, we show that hRAD9 is a nuclear protein, indicating that in this signal transduction pathway, hRAD9 is physically proximal to the upstream DNA damage signal, rather than to the downstream, cytoplasmic, cell cycle machinery.

Introduction

The eukaryotic cell cycle consists of a number of tightly regulated events whose precise order ensures that the important tasks of DNA replication and cell division occur with high fidelity. Cells maintain the order of these events by making later events dependent on the successful completion of earlier events. This dependancy is enforced by cellular mechanisms called checkpoints (Weinert et al. 1988; Weinert et al. 1990). The DNA damage (G2) and DNA replication (S-phase) checkpoints arrest eukaryotic cells at the G2/M transition in the presence of damaged or incompletely replicated DNA, respectively (Weinert and Hartwell 1988; Enoch et al. 1990; Weinert and Hartwell 1990; al-Khodairy et al. 1992; Enoch et al. 1992; Rowley et al. 1992; al-Khodairy et al. 1994). This arrest provides time for the cell to repair damage or complete replication prior to entry into mitosis.

Evidence indicates that in the fission yeast *Schizosaccharomyces pombe*, the ultimate target of the G2 checkpoint signals is the tyrosine 15 residue of the cyclin dependent kinase Cdc2 (Enoch and Nurse 1990; O'Connell et al. 1997; Rhind et al. 1997). Phosphorylation of this residue is regulated primarily by the Cdc25 phosphatase and the Wee1 protein kinase, and the activity of these enzymes is regulated in turn by the kinases Chk1 and Cds1, respectively (Walworth et al. 1993; Furnari et al. 1997). Chk1 is only required for the DNA damage checkpoint (Walworth et al. 1993) and functions by phosphorylating and inhibiting Cdc25, thereby preventing Cdc2 dephosphorylation and mitotic entry (Furnari et al. 1997). When the S phase checkpoint is triggered, activation of Cds1 results in activating phosphorylation of Wee1, which then results in inhibitory phosphorylation of Cdc2 (Boddy et al. 1998). While the mechanistic detail involved in the G2 checkpoints upstream of these proteins is unclear, it is known that a group of six proteins in fission yeast are required for both G2 and S-phase checkpoint control. These proteins are Rad1, Rad3, Rad9, Rad17, Rad26, and Hus1, and are collectively termed the checkpoint rad proteins (al-

Khodairy and Carr 1992; Enoch et al. 1992; Rowley et al. 1992; al-Khodairy et al. 1994). Evidence that these genes are all critical components of both the damage and replication checkpoints is based on observations that the checkpoint rad mutants, unlike wild-type cells, do not block mitotic entry in response to DNA-damaging agents or transient inhibition of DNA synthesis (al-Khodairy and Carr 1992; Enoch et al. 1992; Rowley et al. 1992; al-Khodairy et al. 1994). The checkpoint rads are placed upstream of the Cdc2 regulators in the emerging checkpoint signal transduction pathway because the checkpoint-induced phosphorylation of the Chk1 and Cds1 kinases are dependent on the presence of all of the checkpoint rad proteins (Walworth et al. 1996; Lindsay et al. 1998). More recently, it was shown that Rad1 and Hus1 form a stable complex that is dependant on Rad9, suggesting that these three proteins may exist in a three way complex in fission yeast (Kostrub et al. 1998).

Many of the genes involved in the G2 checkpoint pathways are conserved between humans and yeast. Human homologs of all of the fission yeast checkpoint rads, except Rad26, have been identified, suggesting that the fission yeast G2 checkpoint signalling mechanism may be similar to that of humans (Cimprich et al. 1996; Lieberman et al. 1996; Kostrub et al. 1998; Parker et al. 1998; Udell et al. 1998). In accordance with this hypothesis, Chk2, the human equivalent of *S.pombe* Cds1 protein kinase, has recently been shown to block Cdc2-regulated mitotic entry in response to G2 checkpoint activation, by phosphorylating Cdc25C (Matsuoka et al. 1998). Furthermore, this response is dependent on ATM, a human homolog of fission yeast Rad3 (Savitsky et al. 1995; Savitsky et al. 1995). Therefore, the human equivalents of the checkpoint rads appear to be functioning upstream of the Cdc2 regulatory machinery, as they do in fission yeast.

Here, we identify further conservation between the fission yeast and human G2 checkpoints by demonstrating that human homologs of *S.pombe* checkpoint rads, hRAD1, hRAD9, and hHUS1, physically interact with one another *in vivo*. We also show that endogenous hRAD9 is

phosphorylated and that it localizes primarily to the nucleus in unperturbed HeLa and HaCaT cells.

Materials and Methods

Yeast Two Hybrid Library Screen

hRAD9 cDNA was subcloned from pBluescript into the *Sma*I and *Sal*I restriction sites of the GAL4 DNA binding domain pGBT9 vector (Clontech). pGBT9-hRAD9 was then transformed into the budding yeast strain HF7c (Feilotter et al. 1994) according to the manufacturer's instructions. Transformants were plated on synthetic dropout (SD) media minus tryptophan (6.7 g/l DIFCO Yeast Nitrogen Base without Amino Acids, 2% glucose, 0.62 g/l Bio 101 Complete Supplement Mixture minus histidine (-his), leucine (-leu), and tryptophan (-trp), 20 mg/l histidine, 100 mg/l leucine, and 20 g/l DIFCO Bacto-Agar). To ensure that the hRAD9 GAL4 DNA binding domain hybrid construct alone did not activate the *HIS3* and/or *lacZ* reporter genes, colonies were streaked onto the SD agar-trp-his and tested for β-galactosidase activity using a filter assay described in the Clontech Manual. One HF7c colony harboring the pGBT9-hRAD9 vector was picked into 150 ml of SD-trp liquid media and grown to saturation for two days at 30°C. The saturated culture was then diluted by adding 1 l of YTD (10 g/l yeast extract, 20 g/l tryptone, and 20 g/l dextrose) and grown to an OD_{600} of 0.5. These yeast were then transformed, as described by the manufacturer, with 0.5 mg of a directionally cloned HeLa cDNA library in the pGAD-GH GAL4 activation domain vector (Clontech). The transformants were plated on forty-four 15 cm plates containing SD agar-trp-leu-his and incubated at 30°C. To determine the efficiency of the library transformation, serial dilutions of a small aliquot of the transformed yeast were plated on SD agar-trp-leu. After 10 days, approximately 500 colonies grew larger than background on the triple dropout plates. These colonies were subcultured onto SD agar-trp-leu-his + 5 mM 3-aminotriazole (3-AT) and incubated

at 30°C for 2 days, after which 15 positive clones were identified. Plasmid DNA was then prepared from 15 saturated liquid cultures essentially as described by the manufacturer (Clontech). XL1-Blue competent bacteria were then transformed with this DNA and plated on LB agar containing ampicillin. Inserts in pGAD-GH were sequenced using fluorescently labelled SK primer and an automated sequencer (ABI). DNA sequence analysis was performed using the BLAST algorithm (Altschul et al. 1990).

For analysis of individual interactions between hRAD9, hRAD1, and hHUS1, HF7c were simultaneously cotransformed with pGBT9-hHUS1 and pGAD-hRAD1, pGBT9-hRAD9 and pGAD-hHUS1, and pGBT9-hRAD9 and pGAD-hRAD1, as described by the manufacturer (Clontech). Co-transformants were plated on SD agar-trp-leu and incubated at 30°C for 2-3 days. As negative controls, pGBT9 fusion constructs were co-transformed with empty pGAD-GH vector and pGAD fusion constructs were cotransformed with empty pGBT9 vector. As a positive control, a p53-DNA binding domain fusion construct was co-transformed with a pSV40 T antigen-activation domain fusion construct. A single isolated colony from each plate was streaked onto both SD agar-trp-leu and SD agar-trp-leu-his + 5mM 3-AT and grown at 30°C for 2-3 days.

hRAD9 Polyclonal Antibody Preparation and Purification

hRAD9 cDNA was PCR cloned into the *Sma*I and *Bam*HI restriction sites of the pGEX1 bacterial expression vector (Pharmacia). A hRAD9-Glutathione S-transferase (GST) fusion protein was then expressed in *E. coli* and affinity purified on Glutathione Sepharose (Pharmacia) according to previously described methods (Frangioni et al. 1993). α-hRAD9 polyclonal chicken antibodies were generated against this hRAD9 fusion protein (RCH antibodies).

10 mg of purified GST was batch adsorbed to 2 ml of glutathione sepharose for 2 hours at 4°C. Sepharose was washed with 40 volumes of PBS. 2 ml of antibody supernatant was batch

adsorbed with the GST bound glutathione sepharose overnight. Sepharose was subjected to centrifugation and the supernatant harvested.

35 µg of purified GST-hRAD9 protein was subjected to electrophoresis through a 10% acrylamide gel, then electro-blotted onto a nitrocellulose membrane. The protein band was visualized by Ponceau S staining and the band excised and cut into small pieces with a scalpel. Membrane pieces were blocked overnight in 1% casein in PBST (PBS + 0.1% Tween 20) at 4°C in a microfuge tube. The membane was then washed 3 times for 5 minutes each in PBST. 1 ml of pre-cleared antibody supernatant was added to the membrane pieces and rocked at 4°C for 4 hours. The supernatant was removed and the membrane was washed 2 times rapidly and once for 15 minutes with PBST. The tube was centrifuged briefly and all traces of the wash were removed. The antibody was eluted from membrane with 300 µl of 0.2 M glycine pH 2.8. A second elution with 100 µl of glycine was pooled with the first and the antibody supernatant was neutralized with 0.2 volumes of 1 M Tris pH 8.0.

Co-immunoprecipitation Experiments

Co-immunoprecipitations utilized the myc and flag epitope tags, and for simplicity, proteins expressed with these tags are denoted by a subscripted m or f, respectively. hRAD1 cDNA was amplified by PCR and cloned into the *Xba*I/*Eco*RI restriction sites of the mammalian expression vector, pyDF31 (Gift of Dr. David LeBrun), in frame with one copy of the flag epitope. hRAD9 cDNA was PCR cloned into the *Xba*I/*Xho*I restriction sites of the pCS2-MT, a mammalian expression vector with 6 copies of the myc epitope (Rupp et al. 1994; Turner et al. 1994). A hHUS1-myc fusion construct was generated by PCR amplifying hHUS1 cDNA and cloning it into the pCS2-MT vector. The constructs used to express the negative controls HLF_f and $Fer\Delta N_m$ constructs were gifts of Dr. David LeBrun and Dr. Peter Greer, respectively.

COS-1 cells that were approximately 50% confluent in 10 cm tissue culture plates were transiently co-transfected with 24 µg each of the indicated constructs using lipofectin reagent (SIGMA) according to the manufacturers instructions. Cells were then washed twice with 10 ml of sterile PBS, and 10 ml of complete DMEM was added (DMEM + 10% fetal bovine serum). Transfected cells were cultured at 37°C in a 5 % CO_2 atmosphere for 48 hours. Cells were lysed directly on the plate in mammalian cell lysis solution (50 mM Tris-Cl pH 8.0, 150 mM NaCl, 0.5% NP40, 1 mM Na_3VO_4, 1 mM PMSF, 20 µg/ml aprotinin, 10 µg/ml leupeptin). Lysates were passed through 18 and then 23 gauge syringes several times to shear genomic DNA, incubated on ice for 30 minutes, and centrifuged at 16,000 x g to remove any insoluble material. Each co-transfected cell lysate was split into two equal portions. To one set, lysates were pre-cleared with 35 µl of α-IgY agarose (Promega) on a Nutator at 4°C for 45 minutes, and immunoprecipitated with polyclonal chicken α-hRAD9 antibodies on a Nutator at 4°C for 1 hour. These immune complexes were collected on 35 µl of α-IgY agarose (Promega) at 4°C for 1 hour. To the other set, lysates were pre-cleared with 10 µl protein G-sepharose (Pharmacia) and immunoprecipitated with approximately 1 µg of α-myc 9E10 mouse monoclonal antibody. These immune complexes were collected on 10 µl of protein G-sepharose at 4°C for 1 hour. Both the α-myc and α-hRAD9 immunoprecipitated complexes were collected by centrifugation at 500 x g, washed four times with PBS, and incubated at 100°C for 5 minutes in 50 µl of SDS-PAGE sample buffer (NEB). Following centrifugation at 16,000 x g for 20 minutes, supernatants were electrophoresed through a single 6% acrylamide gel. Protein was transferred to nitrocellulose (0.2 µm pore size, Xymotech) which was blocked in 5% MPBST (PBS + 5% non-fat milk powder + 0.1% Tween 20) at room temperature for 2 hours, and then probed with α-myc 9E10 mouse monoclonal antibody. After extensive washing in PBST, HRP-conjugated anti-mouse secondary antibody was added and the membrane was incubated for 45 minutes at room temperature. Protein antigens were detected by chemiluminescence using the

ECL detection system (Amersham), followed by exposure to X-ray film (Kodak). Three times less α-myc immunoprecipitate sample (12 µl) was loaded onto the gel than α-hRAD9 sample (4 µl). Similarly, Figure 1b, representing the α-myc immunoprecipitate side of the blot was exposed to film for one fifth the time that the α-hRAD9 immunoprecipitate side (Figure 1c).

For the hRAD1/hHUS1 and hRAD9/hRAD1 co-immunoprecipitations, the same methods as described for the hRAD9/hHUS1 co-immunoprecipitations were used, with the following exceptions. All lysates were pre-cleared with 10 µl protein G-sepharose (Pharmacia) on a Nutator at 4°C for 45 minutes. Either α-myc 9E10 monoclonal antibody or α-flag M2 monoclonal antibody was used for immunoprecipitation. Samples were size-fractionated on 10% polyacrylamide gels. Immunoblotting was carried out using α-myc 9E10 mouse monoclonal or α-flag M2 monoclonal antibody, as indicated.

Calf Intestinal Phosphatase Treatments

COS-1 cells were transfected with 24 µg of pCS2-MT-hRAD9 as described previously. Two days after the transfection, cells were harvested and immunoprecipitated with α-myc monoclonal antibody as before. After collecting the immune complexes on protein G-sepharose, beads were washed four times with PBS and resuspended in 200 µl of NEB buffer 3 (50 mM Tris-HCl, 10 mM $MgCl_2$, 100 mM NaCl, and 1 mM DTT) + 1% SDS. Protein was removed from the sepharose beads by heating at 100°C for 5 minutes followed by centrifugation at 16,000 x g. 20 µl of the supernatant was then treated with 30 units of calf intestinal alkaline phosphatase (Promega) in 1x NEB buffer 3 in the presence or absence of 2 mM sodium orthovanadate (Na_3VO_4), for 30 minutes at 37°C. To sufficiently dilute the SDS in the sample, the total volume of the reactions was 200 µl. Both reactions, along with 20 µl of untreated immunoprecipitate, were made up to 1 ml with PBS, and re-immunoprecipitated with α-myc monoclonal antibody, electrophoresed through 6% acrylamide,

and immunoblotted with α-myc monoclonal antibody essentially as above.

Endogenous hRAD9 protein was immunoprecipitated from approximately 9×10^6 HeLa cells with polyclonal chicken α-hRAD9 antibodies essentially as described above. The phosphatase procedure followed was identical to that for exogenous $hRAD9_m$ except samples were electrophoresed through 8% acrylamide and immunoprecipitated and immunoblotted with α-hRAD9 antibodies.

hRAD9 Immunofluorescence

HaCaT or HeLa cells were seeded on coverslips for 1 hour (HeLa) or overnight (HaCaT) at 37°C in 5% CO_2. Cells were washed twice with PBS and fixed with 10% paraformaldehyde for 10 minutes at room temperature. Fixed cells were washed twice more with PBS, covered with methanol, and incubated at -20°C for 20 minutes. Cells were rinsed twice, and then washed for 30 minutes in PBST. PBST + 1% normal goat serum (NGS) was used to block cells at room temperature for 1 hour. Incubation in polyclonal α-hRAD9 chicken antibodies in PBST + 1% NGS for 1 hour at room temperature was followed by two rinses, and one 30 minute wash in PBST. Cells were then incubated in Alexa 488 goat anti-chicken secondary antibody (Molecular Probes) and diluted to 10 µg/ml in PBST + 1 % NGS for 1 hour at room temperature. After two rinses with PBST, and two 10 minute washes in PBS, cells were treated with 200 µg/ml RNase A in 1 % PBS for 1 hour at 37°C. After two rinses and two 5 minute washes in PBST, nuclei were stained with 2 µg/ml propidium iodide in PBS for 5 minutes at room temperature. Cells were rinsed twice and washed once for 10 minutes with PBST. Coverslips were mounted on glass slides and visualized using a Meridian Insight Plus confocal microscope. Images were captured from a cooled Meridian video with a Matrox 1280 frame grabber (Matrox Electronic Systems Ltd.) and pseudo coloured and saved using MCID M4 software (Imaging Research Inc.).

Results

hRAD9 and hHUS1 Physically Interact

We set about to identify proteins interacting with hRAD9 using a two-hybrid screen. The *hRAD9* gene was fused in frame with the *S. cerevisiae* GAL4 DNA binding domain in the pGBT9 vector. This fusion places the GAL4 DNA binding domain at the N-terminus of the full length hRAD9 protein. The construct was transformed into *S. cerevisiae* strain HF7c, and transformants were selected on drop-out media lacking tryptophan. Transformants were isolated and cultured to log phase, then transformed with a cDNA library in which cDNA from HeLa cells had been fused with the GAL4 transactivation domain, in the pGAD-GH vector. Transformants were plated onto double (-leu -trp) or triple (-leu -trp -his) drop-out media to select for the presence of both the bait and a library plasmid, or for protein-protein interaction between bait and prey, respectively. We screened 5.5×10^6 total transformants, and from these identified 15 primary positive clones, each of which was viable on triple drop-out medium in the presence of 5 mM 3-AT. The library plasmids were recovered by transformation into *E. coli*, and the DNA inserts were sequenced. Nine of the 15 isolates contained *hHUS1* cDNA sequences.

To confirm the interaction between hRAD9 and hHUS1, two approaches were taken. First, GAL4 fusion constructs for hRAD9 and hHUS1 were retransformed into *S. cerevisiae* HF7c, and the two-hybrid interaction confirmed (Figure 1a). pGBT9-hRAD9 and pGAD-hHUS1, encoding the entire hHUS1 cDNA sequence, were transformed individually and together into HF7c. In the individual transformations, empty vector of the complementary plasmid was co-transformed. Positive control plasmids fusing p53 and SV40 T-antigen to the GAL4 DNA binding and transactivation domains, respectively, were also co-transformed. Co-transformants were selected

on double (-leu -trp) drop-out media, then subcultured onto triple (-leu -trp -his) drop out media to verify interactions. Neither pGBT9-hRAD9 nor pGAD-hHUS1 could drive expression of the *HIS3* reporter gene (Figure 1a, upper two quadrants). Only when the hRAD9 and hHUS1 fusions were co-transformed together were HIS^+ colonies isolated (Figure 1a, lower right panel), indicating that interaction between the two proteins is required for reconstitution of the GAL4 transcriptional regulator.

The second approach we took to confirm this interaction was to co-immunoprecipitate hRAD9 and hHUS1 proteins exogenously expressed in COS-1 cells (Figure 1b and c). Both hRAD9 and hHUS1 cDNA were subcloned into the pCS2-MT mammalian expression vector. This vector placed six copies of the myc epitope at the C-terminus of hRAD9 and hHUS1. pCS2-MT-hRAD9 and pCS2-MT-hHUS1 were co-transfected into COS-1 cells. Co-transfections with pCS2-MT-FerΔN were also performed to ensure that the co-immunoprecipitation of hHUS1 with hRAD9 was not the result of non-specific interactions involving the myc epitope tag. Cell lysates were immunoprecipitated with α-myc 9E10 monoclonal antibody (Figure 1b) or α-hRAD9 chicken polyclonal antibodies (Figure 1c). Immunoprecipitates were then size-fractionated by SDS-PAGE, transferred to nitrocellulose, and immunoblotted with α-myc monoclonal antibody. hHUS1 co-immunoprecipitated with hRAD9 when cell lysates were incubated with α-hRAD9 antibodies (Figure 1c, lane 1). Although $hHUS1_m$ was exogenously expressed at similar levels in both pCS2-MT-hHUS1 transfected cells (Figure 1b,lanes 1 and 3), in the absence of $hRAD9_m$, $hHUS1_m$ did not immunoprecipitate with polyclonal α-hRAD9 antibodies (Figure 1c, lane 3).

hHUS1 and hRAD1 Physically Interact

Since a Hus1-Rad1 interaction had been previously described in *S.pombe* (Kostrub et al. 1998), we investigated whether a similar interaction existed between hHUS1 and hRAD1. We co-

transformed pGBT9-hHUS1 and pGAD-hRAD1 into HF7c and looked for activation of the *HIS3* reporter gene by sub-culturing co-transformants on triple dropout media (Figure 2a). The same positive and negative controls were used as before. While neither fusion plasmid on its own was sufficient for growth in the absence of histidine, co-transformation of pGBT9-hHUS1 and pGAD-hRAD1 resulted in viable HIS^+ co-transformants. This suggested that a specific interaction existed between hHUS1 and hRAD1.

To confirm this interaction, exogenously expressed hRAD1 and hHUS1 were co-immunoprecipitated in COS-1 cells (Figure 2b-e) using flag epitope-tagged hRAD1 and myc-epitope tagged hHUS1. HLF_f and $Fer\Delta N_m$ were included as negative controls to ensure the specificity of the interaction. Cells were co-transfected as indicated with $hRAD1_f$ / $hHUS1_m$, HLF_f / $hHUS1_m$, or $hRAD1_f$ / $Fer\Delta N_m$. The cells were harvested 48 hours after transfection, lysed, and immunoprecipitated with either α-flag M2 monoclonal antibody or α-myc 9E10 monoclonal antibody. Two aliquots from each sample were electrophoresed through two identical polyacrylamide gels, one of which was used for an α-flag western blot and the other for an α-myc western blot. Although exogenous $hRAD1_f$ protein levels were approximately equivalent in both pyDF31-hRAD1 transfections (Figure 2b, lanes 1 and 3), $hRAD1_f$ immunoprecipitated only with $hHUS1_m$ (Figure 2e, lane 1) and not $Fer\Delta N_m$. (Figure 2e, lane 3). Similarly, $hHUS1_m$ immunoprecipitated with $hRAD1_f$ (Figure 2c, lane 1) but not HLF_f (Figure 2c, lane 2). Together, these results verify the existence of a specific physical interaction between hHUS1 and hRAD1.

hRAD9 and hRAD1 Physically Interact

Having observed the two interactions described above, it seemed logical to explore the association status of hRAD9 and hRAD1. Using the pGBT9-hRAD9 and pGAD-hRAD1 GAL4 fusion constructs, we repeated the yeast two-hybrid experiment described above (Figure 3a). Despite

growth of the p53/pSV40 T-Ag positive control (Figure 3a, lower left quadrant), co-expression of hRAD9 and hRAD1 fusions failed to assemble a functional GAL4, and hence did not produce viable yeast in the absence of histidine (Figure 3a, lower right quadrant). Therefore, while the yeast two-hybrid system demonstrated interactions between hHUS1 and hRAD9, and hHUS1 and hRAD1, it showed no interaction between hRAD9 and hRAD1.

To confirm this result, we examined the ability of hRAD9 and hRAD1 to co-immunoprecipitate in COS-1 cells (Figure 3b-e). $hRAD9_m$ and $hRAD1_f$ were exogenously expressed either together, or separately with HLF_f or $Fer\Delta N_m$, as described above. Neither hRAD1 nor hRAD9 protein expression levels varied significantly between different transfections (Figure 3b lanes 1 and 3; and 3d lanes 1 and 2). Contrary to the yeast two-hybrid data, $hRAD9_m$, but not $Fer\Delta N_m$, immunoprecipitated with $hRAD1_f$ (Figure 3c, lanes 1 and 3) and $hRAD1_f$, but not HLF_f, immunoprecipitated with $hRAD9_m$ (Figure 3e, lanes 1 and 2). Therefore, while hRAD1 and hRAD9 show no interaction in the two-hybrid, they do specifically co-immunoprecipitate with each other when exogenously expressed in COS-1 cells.

hRAD9 is Phosphorylated in Undamaged Cells

From the earliest immunoprecipitations we performed using antibodies directed against either native, or epitope tagged hRAD9 (Figures 1 and 3), we noted multiple discrete bands, the smallest of which corresponded to the predicted size of hRAD9 (Lieberman et al. 1996). We went on to determine that these bands are the result of phosphorylation. To test our hypothesis that these multiple bands were the result of phosphorylation, we transfected COS-1 cells with our $hRAD9_m$ expressing construct, and harvested the cells 48 hours later. The cells were lysed and immunoprecipitated with 9E10 monoclonal antibody directed against the myc epitope. Immunoprecipitates were either untreated, or treated with calf intestinal phosphatase (CIP) in the

presence or absence of sodium orthovanadate. Samples were then subjected to SDS polyacrylamide gel electrophoresis, transferred to nitrocellulose, and immunoblotted with α-myc monoclonal antibodies. Figure 4a lane 1 shows the multiple banding pattern of $hRAD9_m$ in immunoblots, similar to that seen in Figures 1 and 3. Treatment with CIP causes the slower migrating bands to disappear, leaving only the fastest form. This effect can be alleviated by the phosphatase competitor sodium orthovanadate, confirming that the slower migrating bands are the result of multiple phosphorylation states of $hRAD9_m$.

We have also demonstrated that the phosphorylation of $hRAD9_m$ is due neither to the over-expression of the protein in COS-1 cells, nor to the myc epitope tag. We did this using polyclonal chicken antibodies directed against hRAD9 that are of sufficient sensitivity and specificity to detect endogenous hRAD9 in HeLa cells. Essentially the same experiment as above was performed, with the exception that endogenous hRAD9 was detected by polyclonal α-hRAD9 antibodies. In this case, only a single slower migrating band was observed (Figure 4b, lane 1). Also, by contrast with the over-expressed hRAD9 from COS-1 cells, most of the hRAD9 in HeLa cells is phosphorylated. The hRAD9 can be converted to the faster migrating, de-phosphorylated form by treatment with CIP, and this reaction is sensitive to the phosphatase inhibitor sodium orthovanadate (Figure 4b, lanes 2 and 3), indicating that endogenous hRAD9 is phosphorylated in HeLa cells.

hRAD9 is a Nuclear Protein

To determine where hRAD9 localizes in the cell, we used immunofluorescence with a primary polyclonal α-hRAD9 chicken antibody, and a fluorescently labelled secondary anti chicken antibody. The hRAD9 antibodies are able to specifically detect endogenous hRAD9, as evidence by Figure 4b. We used both early log phase HeLa cells, and near confluent HaCaT cells in this study. The location of the Alexa 488 goat α-chicken secondary is represented in green in Figure

5, panel a. The specificity of the secondary antibody is demonstrated by the absence of signal in the absence of primary α-hRAD9 antibodies (Figure 5a; bottom row). Propidium iodide (PI) staining was used to determine the location of the nucleus (Figure 5b), and the images from Figure 5 panels a and b are superimposed in panel c. Corresponding light microscope images are presented in Figure 5d, and superimposed with the fluorescent staining in Figure 5e. The cellular membranes are clearly visible in the HeLa cells, and hRAD9 staining is confined to the nucleus. Similarly, in the confluent HaCaT cells, all hRAD9 staining is nuclear. In both cases the staining is punctate.

Discussion

We have demonstrated three interactions between three human checkpoint rad proteins, hRAD1, hRAD9, and hHUS1. In all cases, these interactions were substantiated using both the yeast two-hybrid system and by co-immunoprecipitation, except for hRAD1 and hRAD9 which did not interact in the yeast two-hybrid, but did co-immunoprecipitate when exogenously expressed in COS-1 cells. The original observation that led to this work was that hRAD9 interacted with hHUS1 in a two-hybrid screen. Nine of 15 interactions isolated in the screen that used hRAD9 as bait were hHUS1. It is interesting to note that hRAD1 was not among the remaining isolates, which are still being characterized. However, the observation that hRAD1 and hRAD9 show no interaction in the two-hybrid had been made previously (Parker et al. 1998). It now appears that this interaction may be dependant on factors that are absent in budding yeast, since hRAD1 and hRAD9 specifically co-immunoprecipitate in COS-1 cells. Such factors may include a budding yeast equivalent of hHUS1, the existence of which seems unlikely considering that no homologs have been identified based on sequence. Alternatively, the N-terminal GAL4 domain of the fusion proteins may result in a conformational change that prevents association of these two proteins. This hypothesis is

supported by our observation that reversing the orientation of the hRAD9/ hHUS1 and hRAD1/ hHUS1 GAL4 fusions, abolishes the *HIS3* reporter gene activation (data not shown). Furthermore, an N-terminal myc tagged version of fission yeast Hus1 has been shown to function as a dominant negative allele (Kostrub et al. 1997). Future use of dominant negative fusions involving human proteins could prove invaluable in uncovering the mechanistic details involved in checkpoint signalling.

It has been shown in fission yeast that Hus1 and Rad1 interact, and that this interaction is dependant on the presence of Rad9, as interaction does not occur in a *rad9* null background (Kostrub et al. 1998). Our data offer strong evidence that such a complex also exists in humans, though it may be assembled differently. While we have only demonstrated pairwise interactions between the three human checkpoint proteins, the simplest explanation of this and the yeast data together is that a three way complex exists between hRAD1, hRAD9, and hHUS1. We can not rule out the possibility that the observed hRAD1-hHUS1 interaction described here are bridged by DDC1, the S. cerevisiae homolog of hRAD9 (Longhese et al. 1997; Paciotti et al. 1998), or by and endogenous monkey homolog of hRAD9 in COS-1 cells. Such evidence will ultimately have to be achieved using hRAD9 null cell lines. Further, with the highly similar phenotypes observed in all of the fission yeast checkpoint rad mutants, and considering recent data demonstrating an interaction between hRAD1 and hRAD17 (Parker et al. 1998), and that ATR, a human homolog of fission yeast Rad3, exists predominantly as part of a high molecular weight complex (Wright et al. 1998), the potential for a multi-protein complex involving all of the checkpoint rad proteins must not be overlooked.

We have also shown that both exogenous and endogenous hRAD9 is phosphorylated at multiple sites. Considering that *S.cerevisiae* DDC1 and *S.pombe* Hus1 both appear to be phosphorylated in response to DNA damage (Kostrub et al. 1997; Paciotti et al. 1998),

phosphorylation is an integral component of checkpoint signalling. To determine if checkpoint activation affects hRAD9 phosphorylation, we investigated whether γ radiation or hydroxyurea could induce a change in the migration pattern of endogenous hRAD9 on a western blot. Neither a 4 Gy dose of gamma radiation, nor incubation in 0.1 mM hydroxyurea for up to 24 hours affected the migration of endogenous hRAD9 from HaCaT cells, though hRAD9 is already highly phosphorylated in these cells. We can not rule out the possibility that ongoing replication or the presence of endogenous DNA damage may be inducing hRAD9 phosphorylation in the absence of exogenous signals. It is worth noting that phosphorylation is not an absolute requirement for association of hRAD9 and hRAD1, as a hRAD1 immunoprecipitation will co-immunoprecipitate all forms of hRAD9, though the most highly phosphorylated forms were preferentially co-precipitated (Figure 3).

Finally, we have investigated the sub-cellular localization of hRAD9, and we have shown that hRAD9 is a nuclear protein (Figure 5). This observation was not a foregone conclusion, as the start of the checkpoint signal transduction pathway is nuclear (DNA damage), while the end is cytoplasmic (the cell cycle machinery). Unlike hRAD1, which has been shown to be present mainly in a diffuse pattern in the nucleus (Freire et al. 1998), the staining pattern of hRAD9 within the nucleus shows discrete areas of intense staining. It will be interesting to further characterize the nature of these foci, including determining what other proteins are present, and whether DNA synthesis, either replicative or unscheduled is occurring in these regions.

The reason for the current intense interest in cell cycle checkpoint control is the association of defects in checkpoint control with human cancers. Genomic instability is a common feature accompanying checkpoint loss, regardless of which checkpoint is compromised, and whether or not the cell is subjected to exogenous stresses (Weinert and Hartwell 1990; Livingstone et al. 1992; Yin et al. 1992). A great deal of evidence now links genomic instability with the multi-step origin

of human cancer (Loeb 1991; Hartwell 1992; Meyn 1995; Smith et al. 1995; Thrash-Bingham et al. 1995; Tlsty et al. 1995; Loeb et al. 1996; Perucho 1996). The number of checkpoint control genes which act as tumour suppressors under normal circumstances is growing, and currently includes *p53* (Malkin et al. 1990; Kastan et al. 1992; Kuerbitz et al. 1992), *ATM* (Savitsky et al. 1995; Savitsky, Sfes et al. 1995; Xu et al. 1996), and *hBUB1* (Cahill et al. 1998). While none of the checkpoint rad proteins has yet been shown to act as a tumour suppressor, several have been mapped to regions associated with loss of heterozygosity in human tumours, which is indicative of the presence of tumour suppressing genes (Lieberman et al. 1996; Parker et al. 1998; Parker et al. 1998). Also, genomic instability has been associated with G2 checkpoint deficiency in budding yeast rad9 mutants (Weinert and Hartwell 1990). Ultimately, the work reported here will shed light on the mechanistic details of how genomic stability is maintained by the G2 and S phase checkpoints.

Acknowledgements

The authors would like to thank Dr. Peter Greer and Dr. David LeBrun for providing plasmids used in this work. We would also like to thank Jennifer Pelley for technical assistance, and Lee Fraser and Deborah Greer for critically reading the manuscript. SD is a Cancer Care Ontario Scientist, and this work was supported by Medical Research Council of Canada Grant MT-14352 and National Institutes of Health Grant ES07940-01A1 to SD. The confocal microscope used in this work is partially supported by Medical Research Council of Canada Equipment Maintenance Grant MT-7827. RPStO is the recipient of a Queen's University Graduate Award. CMU is the recipient of US Army Breast Cancer Research Studentship DAMD17-98-1-8080.

References

al-Khodairy, F. and A.M. Carr (1992). "DNA repair mutants defining G2 checkpoint pathways in *Schizosaccharomyces pombe*." EMBO J **11**: 1343-50.

al-Khodairy, F., E. Fotou, K.S. Sheldrick, D.J. Griffiths, A.R. Lehmann and A.M. Carr (1994). "Identification and characterization of new elements involved in checkpoint and feedback controls in fission yeast." Mol Biol Cell **5**: 147-60.

Altschul, S.F., W. Gish, W. Miller, E.W. Myers and D.J. Lipman (1990). "Basic local alignment search tool." J Mol Biol **215**: 403-10.

Boddy, M.N., B. Furnari, O. Mondesert and P. Russell (1998). "Replication checkpoint enforced by kinases Cds1 and Chk1." Science **280**(5365): 909-12.

Cahill, D.P., C. Lengauer, J. Yu, G.J. Riggins, J.K. Willson, S.D. Markowitz, K.W. Kinzler and B. Vogelstein (1998). "Mutations of mitotic checkpoint genes in human cancers." Nature **392**(6673): 300-3.

Cimprich, K.A., R.B. Shin, C.T. Keith and S.L. Schreiber (1996). "cDNA cloning and gene mapping of a candidate human cell cycle checkpoint protein." Proc. Natl. Acad. Sci. USA **93**: 2850-2855.

Davey, S., C.S. Han, S.A. Ramer, J.C. Klassen, A. Jacobson, A. Eisenberger, K.M. Hopkins, H.B. Lieberman and G.A. Freyer (1998). "Fission yeast rad12+ regulates cell cycle checkpoint control and is homologous to the Bloom's syndrome disease gene." Mol. Cell. Biol. **18**: 2721-2728.

Ellis, N.A., J. Groden, T.Z. Ye, J. Straughen, D.J. Lennon, S. Ciocci, M. Proytcheva and J. German (1995). "The Bloom's syndrome gene product is homologous to RecQ helicases." Cell **83**: 655-66.

Enoch, T., A.M. Carr and P. Nurse (1992). "Fission yeast genes involved in coupling mitosis to completion of DNA replication." Genes Dev **6**: 2035-46.

Enoch, T. and P. Nurse (1990). "Mutation of fission yeast cell cycle control genes abolishes dependence of mitosis on DNA replication." Cell **60**: 665-73.

Feilotter, H.E., G.J. Hannon, C.J. Ruddell and D. Beach (1994). "Construction of an improved host strain for two hybrid screening." Nucleic Acids Res **22**: 1502-3.

Frangioni, J.V. and B.G. Neel (1993). "Solubilization and purification of enzymatically active glutathione S- transferase (pGEX) fusion proteins." Anal Biochem **210**(1): 179-87.

Freire, R., J.R. Murguia, M. Tarsounas, N.F. Lowndes, P.B. Moens and S.P. Jackson (1998). "Human and mouse homologs of Schizosaccharomyces pombe rad1(+) and Saccharomyces cerevisiae RAD17: linkage to checkpoint control and mammalian meiosis." Genes Dev **12**(16): 2560-73.

Furnari, B., N. Rhind and P. Russell (1997). "Cdc25 mitotic inducer targeted by chk1 DNA damage checkpoint kinase." Science **277**(5331): 1495-7.

Hartwell, L. (1992). "Defects in a cell cycle checkpoint may be responsible for the genomic

instability of cancer cells." Cell **71**: 543-6.

Kastan, M.B., Q. Zhan, W.S. el-Deiry, F. Carrier, T. Jacks, W.V. Walsh, B.S. Plunkett, B. Vogelstein and A.J. Fornace, Jr. (1992). "A mammalian cell cycle checkpoint pathway utilizing p53 and *GADD45* is defective in ataxia-telangiectasia." Cell **71**: 587-97.

Kostrub, C.F., F. al-Khodairy, H. Ghazizadeh, A.M. Carr and T. Enoch (1997). "Molecular analysis of hus1+, a fission yeast gene required for S-M and DNA damage checkpoints." Mol Gen Genet **254**(4): 389-99.

Kostrub, C.F., K. Knudsen, S. Subramani, T. Enoch, C.F. Kostrub, K. Knudsen, S. Subramani and T. Enoch (1998). "Hus1p, a conserved fission yeast checkpoint protein, interacts with Rad1p and is phosphorylated in response to DNA damage." EMBO JOURNAL **17 (7)**: 2055-2066.

Kuerbitz, S.J., B.S. Plunkett, W.V. Walsh and M.B. Kastan (1992). "Wild-type p53 is a cell cycle checkpoint determinant following irradiation." Proc Natl Acad Sci U S A **89**: 7491-5.

Lieberman, H.B., K.M. Hopkins, M. Nass, D. Demetrick and S. Davey (1996). "A human homolog of the *Schizosaccharomyces pombe rad9*$^{+}$ checkpoint control gene." Proc. Natl. Acad. Sci. USA **93**: 13890-13895.

Lindsay, H.D., D.J. Griffiths, R.J. Edwards, P.U. Christensen, J.M. Murray, F. Osman, N. Walworth and A.M. Carr (1998). "S-phase-specific activation of Cds1 kinase defines a subpathway of the checkpoint response in Schizosaccharomyces pombe." Genes Dev **12**(3): 382-95.

Livingstone, L.R., A. White, J. Sprouse, E. Livanos, T. Jacks and T.D. Tlsty (1992). "Altered cell cycle arrest and gene amplification potential accompany loss of wild-type p53." Cell **70**: 923-35.

Loeb, L.A. (1991). "Mutator phenotype may be required for multistage carcinogenesis." Cancer Res **51**: 3075-9.

Loeb, L.A. and F.C. Christians (1996). "Multiple mutations in human cancers." Mutat Res **350**: 279-86.

Longhese, M.P., V. Paciotti, R. Fraschini, R. Zaccarini, P. Plevani and G. Lucchini (1997). "The novel DNA damage checkpoint protein ddc1p is phosphorylated periodically during the cell cycle and in response to DNA damage in budding yeast." Embo J **16**(17): 5216-26.

Malkin, D., F.P. Li, L.C. Strong, J.F. Fraumeni, Jr., C.E. Nelson, D.H. Kim, J. Kassel, M.A. Gryka, F.Z. Bischoff, M.A. Tainsky and S.H. Friend (1990). "Germ line *p53* mutations in a familial syndrome of breast cancer, sarcomas, and other neoplasms." Science **250**: 1233-8.

Matsuoka, S., M. Huang and S.J. Elledge (1998). "Linkage of ATM to cell cycle regulation by the chk2 protein kinase." Science **282**(5395): 1893-7.

Meyn, M.S. (1995). "Ataxia-telangiectasia and cellular responses to DNA damage." Cancer Res **55**: 5991-6001.

O'Connell, M.J., J.M. Raleigh, H.M. Verkade and P. Nurse (1997). "Chk1 is a wee1 kinase in the

G2 DNA damage checkpoint inhibiting cdc2 by Y15 phosphorylation." Embo J **16**(3): 545-54.

Paciotti, V., G. Lucchini, P. Plevani and M.P. Longhese (1998). "Mec1p is essential for phosphorylation of the yeast DNA damage checkpoint protein Ddc1p, which physically interacts with Mec3p." Embo J **17**(14): 4199-209.

Parker, A.E., I. Van de Weyer, M.C. Laus, I. Oostveen, J. Yon, P. Verhasselt and W.H. Luyten (1998). "A human homologue of the Schizosaccharomyces pombe rad1+ checkpoint gene encodes an exonuclease." J Biol Chem **273**(29): 18332-9.

Parker, A.E., I. Van de Weyer, M.C. Laus, P. Verhasselt and W.H. Luyten (1998). "Identification of a human homologue of the Schizosaccharomyces pombe rad17+ checkpoint gene." J Biol Chem **273**(29): 18340-6.

Perucho, M. (1996). "Cancer of the microsatellite mutator phenotype." Biol Chem **377**: 675-84.

Rhind, N., B. Furnari and P. Russell (1997). "Cdc2 tyrosine phosphorylation is required for the DNA damage checkpoint in fission yeast." Genes Dev **11**(4): 504-11.

Rowley, R., S. Subramani and P.G. Young (1992). "Checkpoint controls in *Schizosaccharomyces pombe*: *rad1*." EMBO J **11**: 1335-42.

Rupp, R.A., L. Snider and H. Weintraub (1994). "Xenopus embryos regulate the nuclear localization of XMyoD." Genes Dev **8**(11): 1311-23.

Savitsky, K., A. Bar-Shira, S. Gilad, G. Rotman, Y. Ziv, L. Vanagaite, D.A. Tagle, S. Smith, T. Uziel, S. Sfez, M. Ashkenazi, I. Pecker, M. Frydman, R. Harnik, S.R. Patanjali, A. Simmons, G.A. Clines, A. Sartiel, R.A. Gatta, L. Chessa, O. Sandal, M.F. Lavin, N.G.J. Jaspers, A.M.R. Taylor, C.F. Arlett, T. Miki, S.M. Weissman, M. Lovett, F.S. Collins and Y. Shiloh (1995). "A single ataxia telangiectasia gene with a product similar to PI-3 kinase." Science **268**: 1749-53.

Savitsky, K., S. Sfes, D.A. Jagle, Y. Zio, A. Sartiel, F.S. Collins, Y. Shiloh and G. Rotman (1995). "The complete sequence of the coding region of the *ATM* gene reveals similarity to cell cycle regulators in different species." Hum Mol Gen **4**: 2025-2032.

Smith, M.L. and A.J. Fornace, Jr. (1995). "Genomic instability and the role of p53 mutations in cancer cells." Curr Opin Oncol **7**: 69-75.

Thrash-Bingham, C.A., H. Salazar, J.J. Freed, R.E. Greenberg and K.D. Tartof (1995). "Genomic alterations and instabilities in renal cell carcinomas and their relationship to tumor pathology." Cancer Res **55**: 6189-95.

Tlsty, T.D., A. Briot, A. Gualberto, I. Hall, S. Hess, M. Hixon, D. Kuppuswamy, S. Romanov, M. Sage and A. White (1995). "Genomic instability and cancer." Mutat Res **337**: 1-7.

Turner, D.L. and H. Weintraub (1994). "Expression of achaete-scute homolog 3 in Xenopus embryos converts ectodermal cells to a neural fate." Genes Dev **8**(12): 1434-47.

Udell, C.M., S.K. Lee and S. Davey (1998). "*HRAD1* and *MRAD1* encode mammalian homologues

of the fission yeast *rad1*$^+$ cell cycle checkpoint control gene." Nucleic Acids Res. **26**: 3971-3978.

Walworth, N., S. Davey and D. Beach (1993). "Fission yeast chk1 protein kinase links the *rad* checkpoint pathway to *cdc2*." Nature **363**: 368-71.

Walworth, N.C. and R. Bernards (1996). "rad-dependent response of the chk1-encoded protein kinase at the DNA damage checkpoint." Science **271**: 353-6.

Weinert, T.A. and L.H. Hartwell (1988). "The *RAD9* gene controls the cell cycle response to DNA damage in *Saccharomyces cerevisiae*." Science **241**: 317-22.

Weinert, T.A. and L.H. Hartwell (1990). "Characterization of *RAD9* of *Saccharomyces cerevisiae* and evidence that its function acts posttranslationally in cell cycle arrest after DNA damage." Mol Cell Biol **10**: 6554-64.

Wright, J.A., K.S. Keegan, D.R. Herendeen, N.J. Bentley, A.M. Carr, M.F. Hoekstra and P. Concannon (1998). "Protein kinase mutants of human ATR increase sensitivity to UV and ionizing radiation and abrogate cell cycle checkpoint control." Proc Natl Acad Sci U S A **95**(13): 7445-50.

Xu, Y. and D. Baltimore (1996). "Dual roles of ATM in the cellular response to radiation and in cell growth control." Genes Dev **10**(19): 2401-10.

Yin, Y., M.A. Tainsky, F.Z. Bischoff, L.C. Strong and G.M. Wahl (1992). "Wild-type *p53* restores cell cycle control and inhibits gene amplification in cells with mutant *p53* alleles." Cell **70**: 937-48.

Figure Legends

Figure 1. hRAD9 and hHUS1 physically interact. ***a.*** *S. cerevisiae* strain HF7c was transformed with the indicated GAL4 fusion plasmids and plated on media selecting for co-transformants. Single colonies were sub-cultured onto selective media in the presence (left) or absence (right) of histidine. Growth in the absence of histidine is indicative of a protein:protein interaction, as demonstrated by the p53:SV40 T-Ag positive control (lower left quadrant). When pGBT9-hRAD9 and pGAD-hHUS1 were cotransformed separately with the corresponding empty vector, no growth on triple dropout was observed (upper two quadrants). Expression of both hRAD9 and hHUS1 GAL4 fusions were required for viability in the absence of histidine (bottom right quadrant). ***b.-c.*** COS-1 cells were transiently co-transfected with constructs expressing $hRAD9_m$ and $hHUS_m$ (lane 1), $hRAD9_m$ and $Fer\Delta N_m$ (lane 2), or $hHUS1_m$ and $Fer\Delta N_m$ (lane 3). After harvesting, lysates were immunoprecipitated with α-myc 9E10 monoclonal antibody (*b.*) or chicken α-hRAD9 polyclonal antibodies (*c.*), and in both cases were immunoblotted with α-myc 9E10 monoclonal antibody. Specific coimmunoprecipitation of $hRAD9_m$ and $hHUS1_m$ is observed in panel c, lane 1.

Figure 2. hRAD1 and hHUS1 interact specifically. ***a.*** *S cerevisiae* strain HF7c was co-transformed with the indicated GAL4 fusion plasmids and plated on media selecting for co-transformants. Single colonies were then sub-cultured onto selective media in the presence (left) or absence (right) of histidine. Similar to the positive control (lower left quadrant), co-transformation of pGBT9-hHUS1 and pGAD-hRAD1 resulted in growth in the absence of histidine (bottom right quadrant). When either construct was co-transformed separately with the corresponding empty GAL4 vector, no growth on -trp-leu-his media was observed (upper two quadrants). ***b.-e.*** COS-1

cells were transiently cotransfected with constructs expressing $hRAD1_f$ and $hHUS1_m$ (lane 1), HLF_f and $hHUS1_m$ (lane 2), or $hRAD1_f$ and $FER\Delta N_m$ (lane 3). After harvest, lysates were immunoprecipitated with α-flag M2 monoclonal antibody (b. & c.) and then immunoblotted with α-flag (b) or α-myc antibodies (c). Aliquots of the same COS-1 cell lysates were also immunoprecipitated with α-myc 9E10 monoclonal antibody (d. & e.) and immunoblotted with α-myc (d) or α-flag (e) antibodies. Specific co-immunoprecipitation of $hRAD1_f$ and $hHUS1_m$ is observed in panel c, lane 1 and panel e, lane 1.

Figure 3. hRAD9 and hRAD1 co-immunoprecipitate ***a.*** S. cerevisiae strain HF7c was co-transformed with the indicated GAL4 fusion plasmids and plated on media selecting for co-transformants. Single colonies were then sub-cultured onto selective media in the presence (left panel) or absence (right panel) of histidine. While the p53:SV40 T-Ag positive control grew in the absence of histidine (lower left quadrant), expression of both hRAD9 and hRAD1 GAL4 fusions did not result in the formation of HIS^+ yeast colonies (bottom right quadrant). Therefore, no interaction was detectable between these two proteins. ***b.-e.*** COS-1 were transiently cotransfected with constructs expressing $hRAD1_f$ and $hRAD9_m$ (lane 1), HLF_f and $hRAD9_m$ (lane 2), or $hRAD1_f$ and $Fer\Delta N_m$ (lane 3). After harvest, lysates were immunoprecipitated with α-flag M2 monoclonal antibody (b. & c.) and then immunoblotted with α-flag (b) or α-myc antibodies (c), or were immunoprecipitated with α-myc 9E10 monoclonal antibody (d. & e.) and immunoblotted with α-myc (d) or α-flag (e) antibodies. Specific co-immunoprecipitation of $hRAD1_f$ and $hRAD9_m$ is observed in panel c, lane 1 and panel e, lane 1.

Figure 4. hRAD9 is phosphorylated in undamaged cells. ***a.*** COS-1 cells transiently transfected with the construct expressing $hRAD9_m$. Following harvest, lysates were immunoprecipitated with

α-myc 9E10 monoclonal antibody. Fractions of the immunoprecipitate were either treated or not with calf intestinal phosphatase (CIP) in the presence, or absence of orthovanadate (VO_4). Samples were then subjected to western analysis using antibody directed against the myc epitope. CIP treatment resulted in elimination of slower migrating forms of $hRAD9_m$, an effect that was not observed when VO_4 was present. ***b.*** Logarithmically growing HeLa cells were harvested, subjected to western analysis using polyclonal α-hRAD9 antibodies. As in panel *a.*, samples also treated with CIP in the presence or absence of vanadate, as indicated.

Figure 5. hRAD9 is located in the nucleus. Confocal immunofluorescence and light microscopy was performed on <50% confluent HeLa cells and 90% confluent HaCat cells. Cells were fixed and probed with α-hRAD9 chicken polyclonal antibodies, followed by a fluorescently labelled anti-chicken IgY secondary antibody (***a.***). DNA was visualized by staining with propidium iodide (***b.***). Images from *a.* and *b.* were superimposed (***c.***). The cellular borders of the HeLa and confluent HaCaT cells were visualized by light microscopy (***d.***), and the light and fluorescent images were superimposed (***e.***).

a.

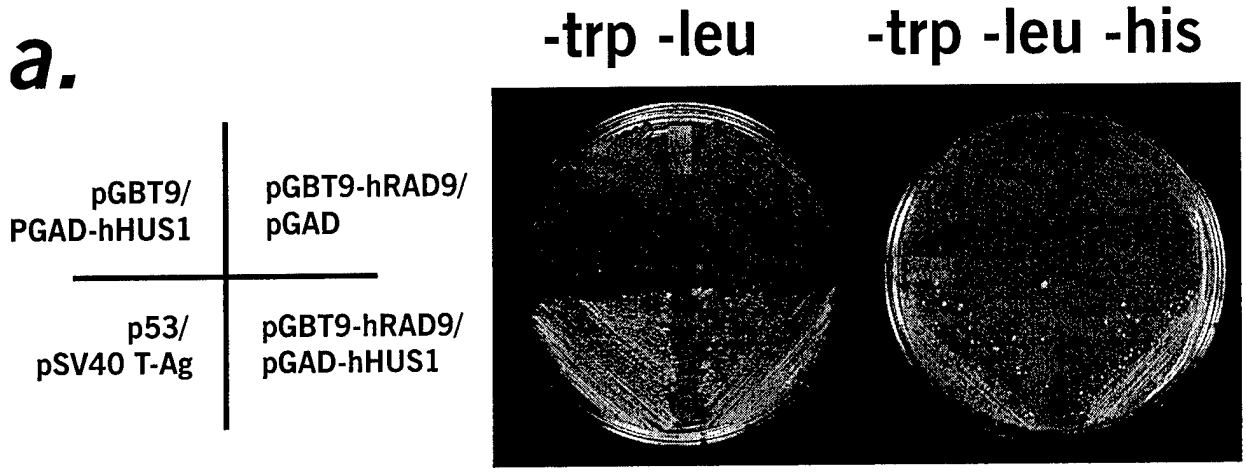
-trp -leu
-trp -leu -his
pGBT9/
PGAD-hHUS1
pGBT9-hRAD9/
pGAD
p53/
pSV40 T-Ag
pGBT9-hRAD9/
pGAD-hHUS1

b.

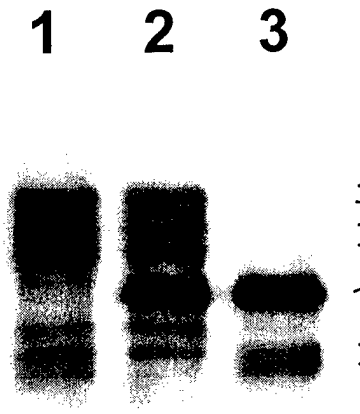
1
2
3

c.


1
2
3

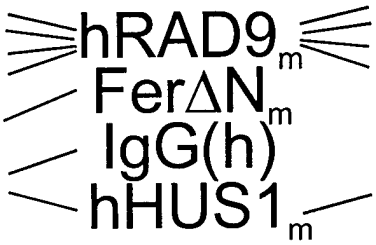
hRAD9m
FerΔNm
IgG(h)
hHUS1m

1.5 inches

1

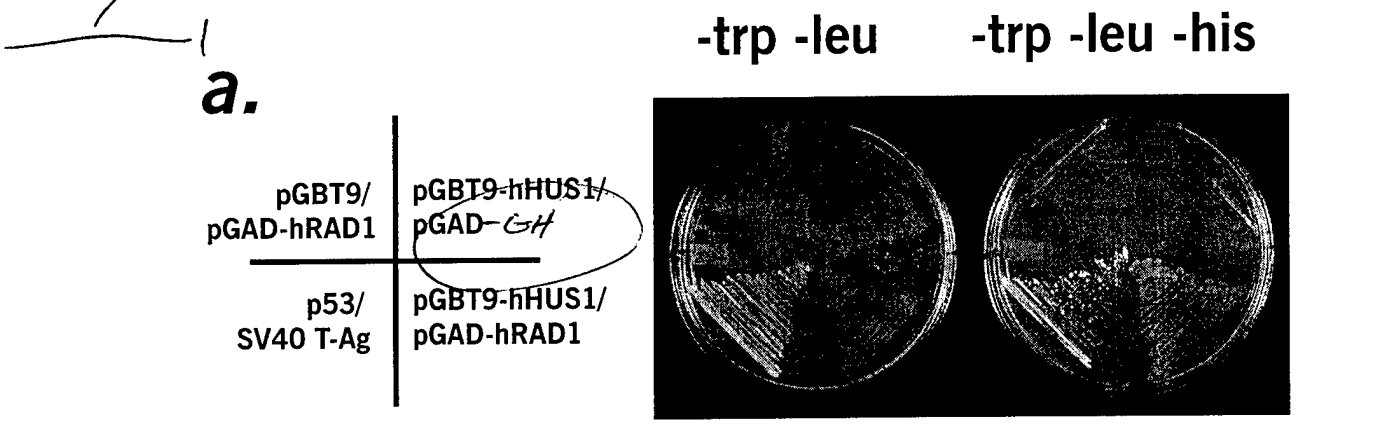
a.
-trp -leu
-trp -leu -his
pGBT9/
pGAD-hRAD1
pGBT9-hHUS1/
pGAD-GH
p53/
SV40 T-Ag
pGBT9-hHUS1/
pGAD-hRAD1
b.
1
2
3
50-
36-
29-
-IgG(h)
-HLF$_f$
-hRAD1$_f$
-IgG(l)
c.
1
2
3
84-
50-
36-
-IgG(h)
-hHUS1$_m$
d.
1
2
3
84-
50-
36-
-FER$_m$
-IgG(h)
-hHUS1$_m$
e.
1
2
3
50-
36-
29-
-IgG(h)
-hRAD1$_f$
-IgG(l)

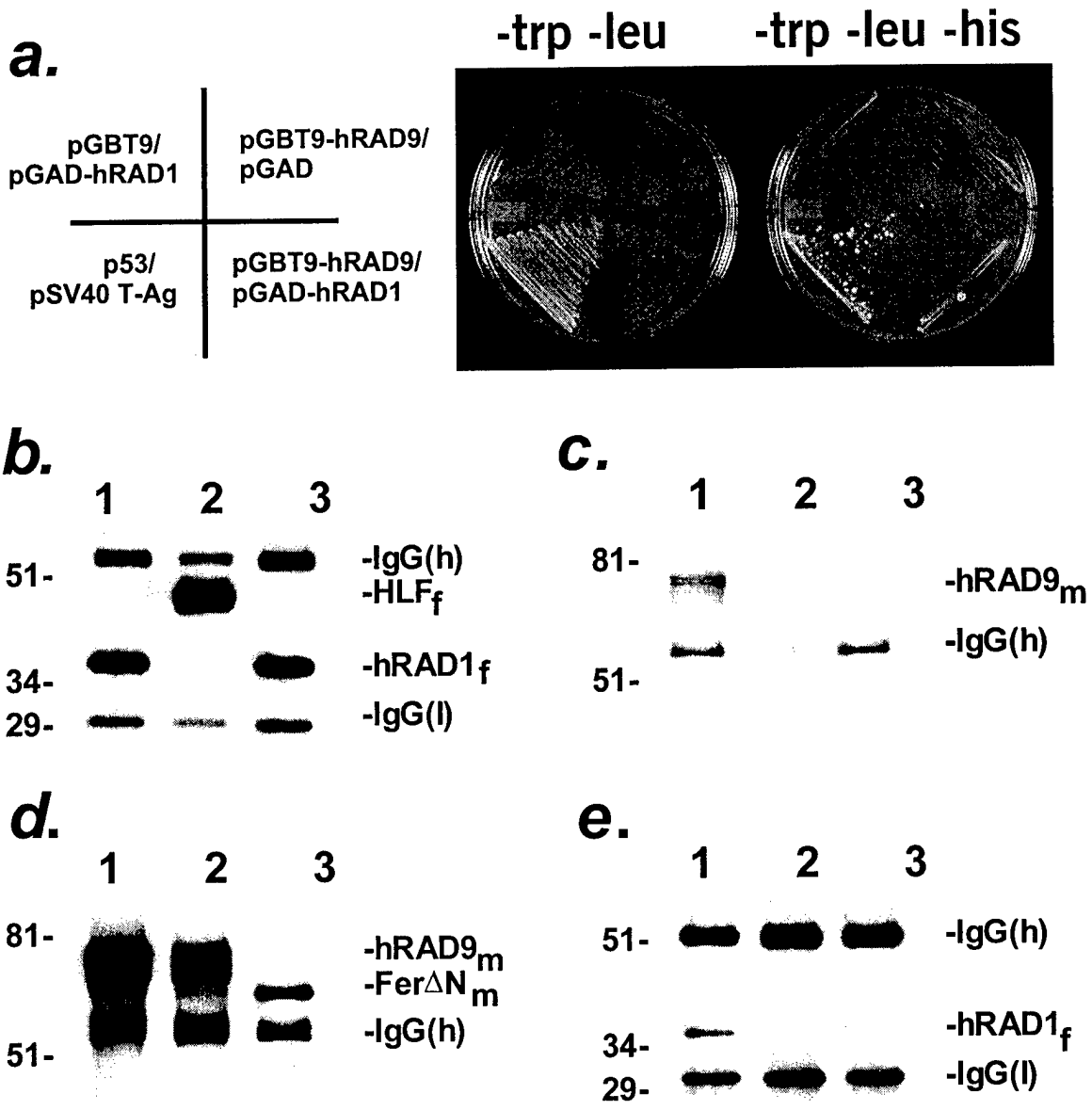
a.
-trp -leu
-trp -leu -his
pGBT9/
pGAD-hRAD1
pGBT9-hRAD9/
pGAD
p53/
pSV40 T-Ag
pGBT9-hRAD9/
pGAD-hRAD1
b.
1
2
3
51-
34-
29-
-IgG(h)
-HLF$_f$
-hRAD1$_f$
-IgG(l)
c.
1
2
3
81-
51-
-hRAD9$_m$
-IgG(h)
d.
1
2
3
81-
51-
-hRAD9$_m$
-FerΔN$_m$
-IgG(h)
e.
1
2
3
51-
34-
29-
-IgG(h)
-hRAD1$_f$
-IgG(l)

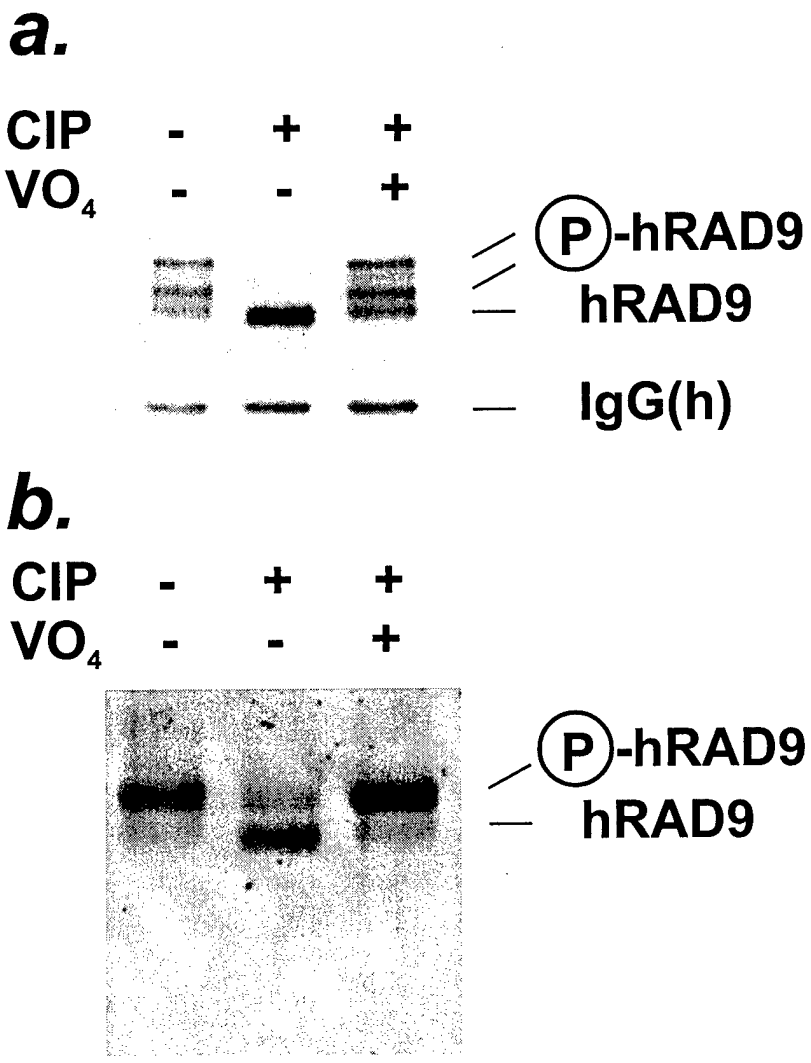
a.
CIP - + +
VO4 - - +
P-hRAD9
hRAD9
IgG(h)
b.
CIP - + +
VO4 - - +
P-hRAD9
hRAD9

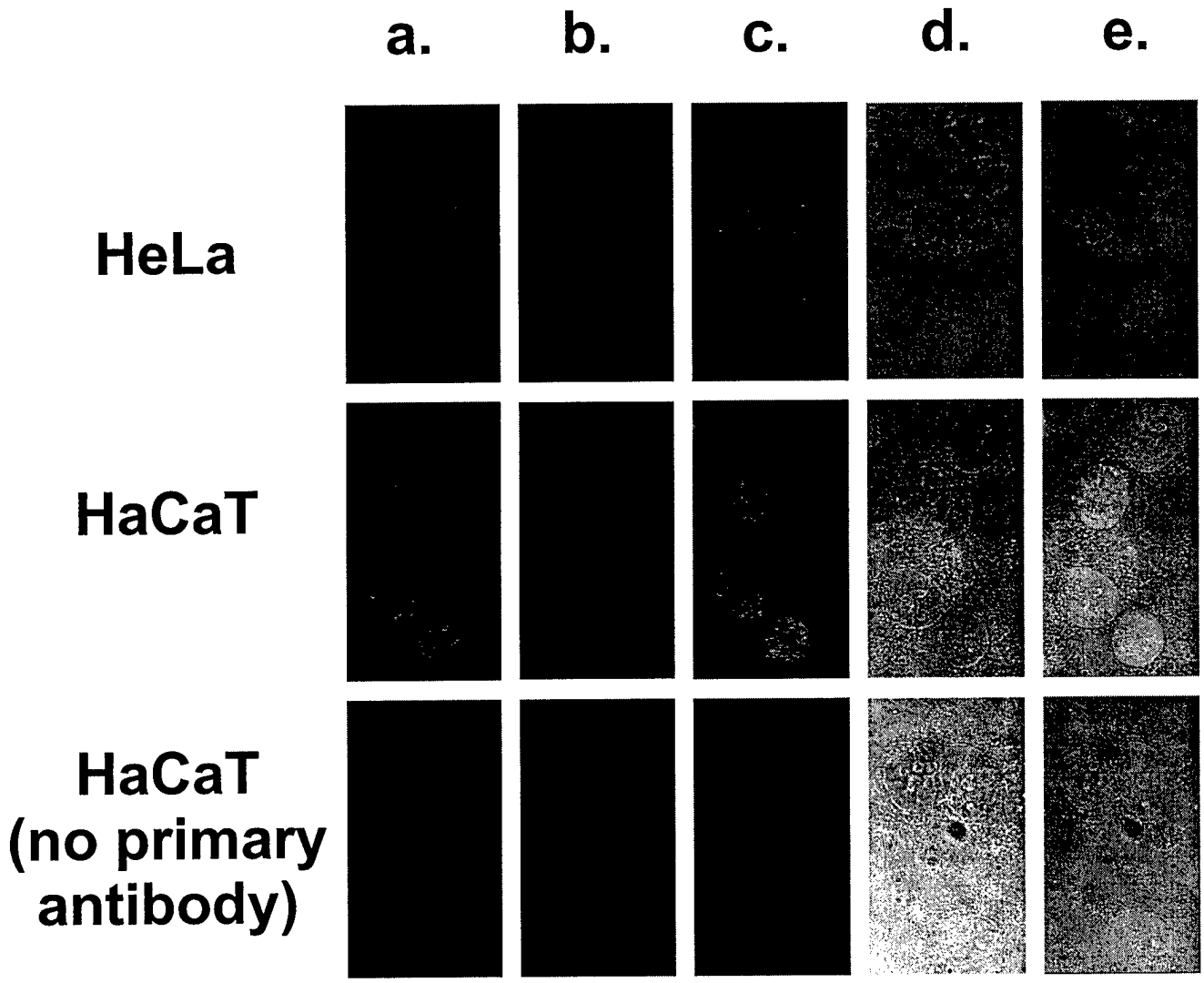
a.
b.
c.
d.
e.
HeLa
HaCaT
HaCaT
(no primary
antibody)